Volume 9, Issue 2, 2019, 3874 - 3883 ISSN 2069-5837

Biointerface Research in Applied Chemistry

www.BiointerfaceResearch.com

https://doi.org/10.33263/BRIAC92.874883

Original Research Article Open Access Journal

Received: 16.02.2019 / Revised: 30.03.2019 / Accepted: 08.04.2019 / Published on-line: 15.04.2019

Reaction of cell membrane bilayers "as a variable capacitor" with G-protein: a reason for neurotransmitter signaling

Thu Thi Pham [1], Majid Monajjemi [1, 2,*], Dung My Thi Dang [1], Fatemeh Mollaamin [1], Chien Mau Dang [1]

[1]Institute for Nanotechnology (INT), Vietnam National University - Ho Chi Minh City (VNUHCM), Ho Chi Minh City, Vietnam
[2]Department of chemical engineering, Central Tehran Branch, Islamic Azad University, Tehran, Iran

*corresponding author e-mail address: ***Maj.monajjemi@iauctb.ac.ir***

ABSTRACT

Cell membranes have unique features to store bio-energy in the physiology subjects. This work demonstrates a model of biological capacitors in the phospholipids bilayers membrane including DPPC, DOPG, DOPE, DOPS and DMPC structures. The electron densities profiles, electron localization function (ELF) and local information entropies have been used for studyng the interaction of G-proteins with phospholipid bilayers. The quantum and columbic blockade effects in different sizes and thicknesses of the membrane have also been specifically studied. It has been shown the quantum effect might appear in the small regions of the free spaces through membrane thickness due to the number and variant of phospholipids layer. In addition, based on Heisenberg rule, it has been exhibited the quantum tunneling effects are allowed the micro position while they are not allowed in other shapes of membrane capacitors. Due to the dynamical behavior of the bilayers in the membrane, their capacitances are not fixed which mean they are variable capacitors. Although the G protein successor does not interact to the phospholipid bilayers but stabilizes a true activated situation of the receptor, for stabilizing an activated conformational structure is tightly influenced through the lipidic situation in G proteins in viewpoint of capacitors model. Through an external field the G- protein trance membrane, charges exert forces that can influence the state of the cell membrane. Consequently the charge capacitive susceptibility could resonate with self-induction of helical coils in the (GTP) or (GDP) likes digital switches. These resonances are the main reason for any biological pulses in cell signaling cooperation.

Keywords: *lipid bilayers, variable capacitors, cell membrane capacitors, G-proteins, GTP, GDP.*

1. INTRODUCTION

1.1. G protein membrane interaction

Cell membranes have an accurate structural potential that acts as a platform for the assembling various signal transition routes including additional levels for regulating of cell signaling cooperation. Although this dynamical structure of the cell membrane causes the lipid–lipid and lipid–protein interactions in all sites, meanwhile there is an important interaction of those complexes with the sub-membrane Cyto-skeleton in some places. In addition the micro-domains add further complexity to these kind interactions, as well as the message propagation in component of cell membrane Via G proteins and other proteins. G proteins, known as guanine nucleotide-binding membrane associated proteins, are a group of polypeptides that act such as macro-molecule switches among the component of cells. This action is involved in transmitting signals from several of stimuli outside of the cells towards interior sections. G Proteins are combined of three subunits as names α, β and γ (scheme1). The trimer is located in the cell membrane through several fatty acids such as myristoyl, palmitoyl and prenyl moiety at the N-terminus of the "α" subunit and C-terminus of the γ-subunit, respectively [1]. The activities are regulated via several co-factors that control their abilities for binding to hydrolyze guanosine tri & di-posphate (GTP) or (GDP) like digital switches (0 &1). When it is attached to GTP, is "1" which means "on", and on other hand, when it is attached to GDP, is zero which means "off". The fundamental cyclic diagram of G-protein mechanism both activation and in-activation is shown in scheme 2. The step 1 is the basal state which the α-subunit attached to GDP and in the step2; activation has been done through Ag to the G-protein. Meanwhile a conformational changing has been done in the protein that affects a high-affinity of GTP attaching on the α-subunit.

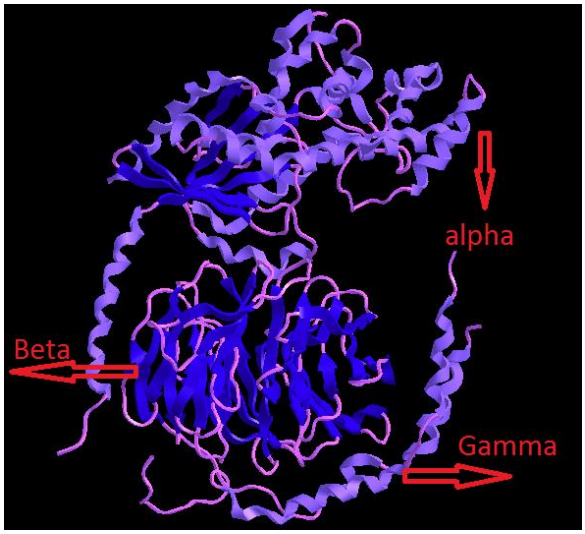

Scheme 1. Structure of hetero-trimetric G protein alpha, beta and gamma in complex.

Due to the concentration of GTP a GTP: GDP nucleotide exchanging appears in the cell membrane which induces a partial dissociation of theα and βγ subunits [2]. In step 3, Theα and βγ sections conjointly or sometimes separately interact with a few effector proteins, for activating or inhibiting theme. The mechanism finally is finished through hydrolysis reaction of α-attached GTP to GDP via the GTP'ase activities of the α-subunit.

Consequently, GDP-bounded to α-subunit re-associate by the βγ-subunits for restoring the initial state and then dissociation of βγ appears in the transduction route [3].

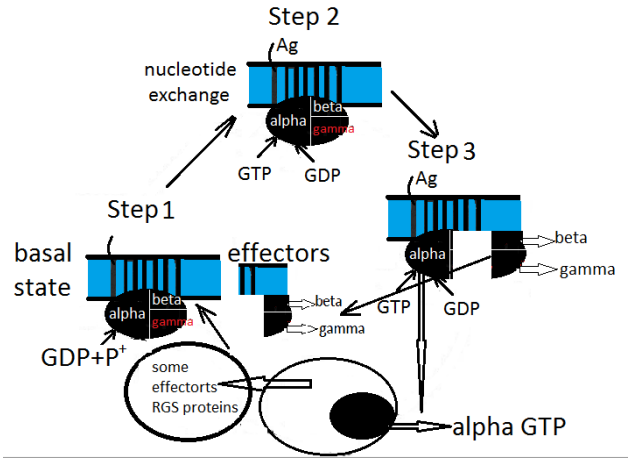

Scheme 2. G-protein mechanism of activation and in-activation

G protein-coupled receptors or GPCRs are the big macromolecule in the ranges of cell membrane receptors for cellular signaling [4]. They are sensitive to the wide ranges of hormones, peptides, ions and photons. Based on ligand bonded over the extra membrane sides, GPCRs has been changed in its conformational structures. The cellular reaction and signaling mechanism is related to the G protein subunits and also the specific coupling of GPCRs such as G_s, G_i, G_q, and G_{12} [5,6]. Through interactions with the trans-membrane receptor (TM3, 5, and 6), the Gα subunit directly attached for achieving to the largest conformational changing in the G protein (exchange of GDP for GTP in the nucleotide binding pocket) [7]. Although from studies on the prototypical GPCR rhodopsin, it is obvious that the phospholipid plays a major role in modulating and signaling [8-10], the membranes in which other GPCRs function have a few diversity in view point of protein composition [11,12]. So, it is important to study the previous observation on the lipid bilayers of rhodopsin to various GPCRs.

1.2. DNA repairing, DNA Stabilities and Aging.

Human aging is related to the agglomeration of deleterious cellular molecules that dramatically affect the functionality of the cells and several tissues in organs. These stochastic agglomerations of cell perturbations induce significant signaling in body towards invalidism and also affect several processes related to de-catabolism, protein unfolding and denaturing, membrane instability and improper cellular replication. Some signals control the effective catabolism of glucose as the first energy sources in the tissue of higher organisms such as brain. A few mutations affect various cellular functions which are dramatically damage of the insulin receptor mechanism and so little caloric intake was extant (insulin resistance was low). So, during increasing age, there are common systems for reduction the ability of the body due to a degradation of the efficiency of ATP-generating. The GPCR groups are the most diverse group of trans-membrane proteins in the human proteomes which have been evolved for providing cell-membrane with incredibly sensitive sensory systems from the photons, chemical & physical phenomenon of several neurotransmitters, hormones and in total micro catabolism [13, 14]. Therefore GPCR sensitivities have allowed cellular pharmacologists for exploiting those complexes signaling mechanism reasonability to fight with

various diseases. GPCRs equip strongly flexibility and a suitable mechanism for the signal transfer of those messages from the receptor and ligands to the intracellular environment. These receptors basically function as ligands-activated guanine nucleotides exchanges factors "GEFs" for hetero-tri-meric G proteins. G proteins activation changes in the tertiary conformation of the hepta-helical segment that is then transmitted to the inside cell via trans-membrane protein's loops and also carboxyl terminal of the receptors. This conformational changes the potential of the receptors for interacting G-proteins and GDP to GTP on theα subunit. The nucleotide exchanging elevates dissociation of the αβγ subunits to the α-GTP and the free βγ subunits which the α-GTP subunit motivates its effectors, phospholipase-C and supplying information about the extracellular volubility to the intracellular.

Moreover Gα and βγ subunits also contain effectors stimulatory activities and progress the G coupling to the receptor. The centered G protein or GPCR signaling is not the only physiologically-relevant signaling and the β-arrestin signaling route and additional drug design avenues may be fruitful. Luttrell exhibited that β-arrestins interact with kinases family and its coupling with beta adrenergic receptors to extra membrane signal-regulated pathways [15]. β-arrestins have been shown for binding wide varieties of signaling macromolecules with GPCR which can occur in parallel, or subsequently to, G protein turnover [16]. In addition β-arrestin, via the β2-adrenergic (β2AR) receptor, causes for increasing DNA damage, p53 decays and the progress of apoptosis [17]. This information confirms that the activation of β2AR might be signal through non-β-arrestin signaling mode; therefore DNA damage repair could be happened.

1.3. Phospholipids binding to the β2AR.

Human β2AR receptor can be reconstruction in high concentration lipo-particles and it has been shown that the β2AR can be reconstituted as a fully functional monomer in HDL [18]. Rosie dawaliby et al. selected [19] the main lipids membranes such as phosphatidylethanolamine (PE), phosphatidylcholine (PC), phosphatidylglycerol (PG), phosphatidylserine (PS) and phosphatidylinositol (PI) among the most abundant type in mammalian membranes for reconstitution of β2R into HDL.

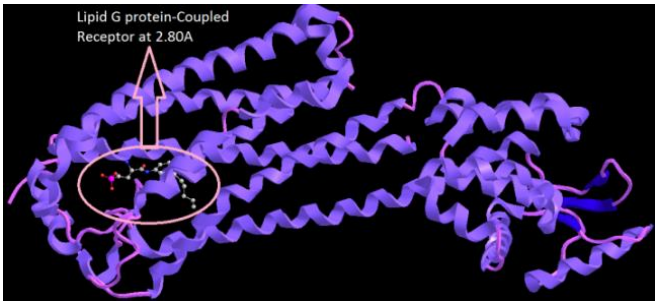

Figure 1. Crystal Structure of Lipid ({(3R)-3-amino-4-[(3-hexylphenyl) amino] -4-oxobutyl}phosphonic acid $C_{16}H_{27}N_2O_4P$) to the G protein-Coupled Receptor at 2.80A.

They exhibited, G protein binds straightly with the membrane phospholipids and thus changes in coupling performance might be due to amended affinities of the G proteins for those phospholipids, altered receptor function, or a combination of both of theme. So, definition the respective contributions might be a

problem and for the β2R, this difficulty can be solved by using nanobody Nb80. It is notable that the G protein successor does not interact to the phospholipid bilayers but stabilizes a true activated situation of the receptor [20]. The capability of Nb80 for stabilizing an activated conformational structure is tightly influenced through the lipidic situation in G proteins [21] (Fig.1).

Interestingly however DOPG provided the suitable activated environment (reaching a λmax shift of 13 nm after 30 min), DOPS did not stabilize the Nb80-bound activated states compare to DOPG. Obviously the negative charge on the head-group DOPS is not suitable for stabilizing the activated conformation.

In viewpoint of the polar head-groups sizes which are (PS ≈ PG < PI), the differences are improbable to arise from transformation in charges densities.

DOPE presented the least suitable environment for Nb80-induced β2AR [19] .Rosie Dawaliby et al. demonstrates [19] that lipids act as modulators of GPCR composition and activity and that these effects are driven through the nature of the head-groups. Both binding approaches and induced conformational testing exhibited that DOPG and DOPS promote β2AR activation, while, DOPE favors the inactivated states.

1.4. Membrane as a capacitor model.

All capacitors are modeled with the same fundamental structures in both classical and quantum approaches. During of appearing different voltages between two plates of a capacitor, an electrical field is produced in the dielectric section which results in the storage of electrical energies in order for producing the mechanical forces between two sides. In the variable capacitors, the capacitances must be intentionally and repeatedly changed, either mechanical or electronically forms. Variable capacitor is usually applied in L/C electronic devices for setting the resonance frequency to tune a radio or changing the reactance for impedance matching in antenna devices. Compare to a capacitor, the structure of a cell membrane can straightly affect its function, such as permeability, signaling and capacitance [22]. The lipid bi-layers in membrane structures are covered on both sides through collection of charged dissolved minerals with a similar function as a conducting metal plate. The exterior phospholipids membrane as instant in mitochondria from mammals and chloroplasts from plants has the capacities for accumulating and storing charges for producing enough energy. Several studies on the phospholipids have been accomplished in viewpoint of exploring properties as cholesterol's impacts, heat capacities, increasing salt densities, correlative lipid motion during diffusions, thickness fluctuations and bilayer undulations. Interaction of trans-membrane-proteins with phospholipids has also been studied through molecular dynamics (MD) simulations. The phospholipids bi-layers themselves are mostly impenetrable for ions and molecules. So, charged ions might cross via special channels in the lipid bilayers which are known as the ion channels. This channel is made of trans-protein-membrane, including aqueous solutions which connect to the inside of the membrane. This channel is able to open and close in response to several signals (Fig.2). The passage of these ions via these channels dedicates the membrane with the electrical conductivities to allow for inside and outside current flows [11]. This is a major function that creates electrical circuits in the biological systems. Therefore, the electro-physiologies and dynamical behaviors of membrane cause the cell to act as the variable capacitors and proteins are considered as electrical resistance. The membranes are interfaces among the cells interior, other proteins as well as the extracellular component that facilitates the adherence and communication with those components as well as other biological section. The usual properties of phospholipids structures enable the membrane components as well as the whole cells to resonance together.

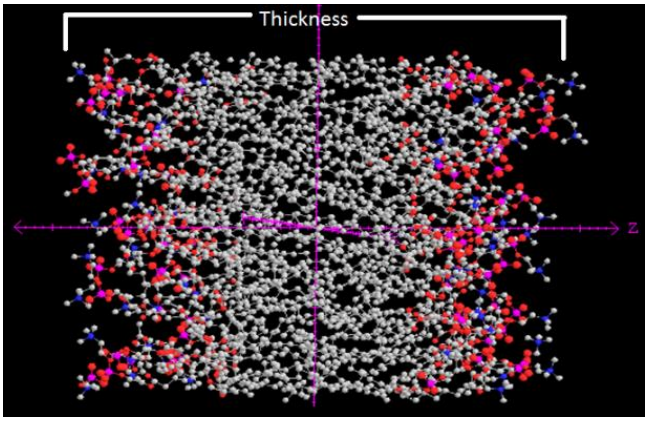

(a)

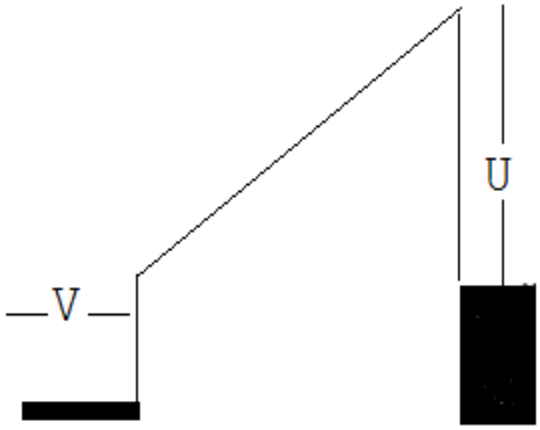

(b)

Figure 2. (a): Structure of a membrane, (b) capacitor, under applied Voltage.

It is suggested by Smith and Choy that the cellular components create the capability to function as electrical resonators [23, 24]. Activating the receptor has various outcome issues such as: increasing the transport of specific molecules or ions from one side to the other side in a thicknesses of cell membrane, inhibiting the enzymes in a metabolic synthesis, activating genes for producing specific proteins, turning off the gene production of other proteins or changing the shape of the cell, from the effector proteins/enzymes with releasing a signal [23]. It is notable that signaling mechanisms are either chemically or resonantly mediated. The signaling should be produced with remote controls through endocrine cells via cells such as macrophages, T-cells and B-cells. The receptors of membrane can also be activated through an electrical field or vibrational resonance with a specific frequency via electro-conformational coupling. The charges distribution in component in membrane receptors might be altered through electrical oscillations from the true frequency, causing the cell receptors to undergo conformational changes. By this study it has been exhibited that the various phospholipids in the cell

membranes work as a variable capacitor during resonating with the G-proteins and related receptors and components such as G_s, G_i, G_q, and G_{12}. They would lead towards alteration/initiation of cell regulation of internal cellular processes. This phenomenon antagonizes any further changing in the current, same as Lenz rule concerning voltage and amperage in the coils in inductors. Simultaneously the conductors are coiled; the magnetic fields are produced by the currents flow expands across adjacent coil turning points. A small changing in the voltages could be lead to the larger uptake of charges and largest capacitive currents. These currents change the induced magnetic fields and also create a few forces which antagonize the changes in the currents. These effects do not occur in the static conditions of DC circuits during the steady currents. Several trans-membrane proteins contain helical coils in G proteins structures which might allow them to electronically function as inductor coils and enable the cells to transiently produce very high electrical voltages.

2. MATERIALS AND METHODS

2.1. Membrane capacitor model.

The phospholipids variable capacitance $C_{membrane}(t)$ has been defined as the amount charges (q) which are stored on two electrodes at the specific membrane's voltages versus of time V_{mem} (*t*). Exactly, due to the Nano scale in a cell membrane, quantum electrical phenomenon must be taken into calculation. In case of very thickness of membrane structures, these configurations indicate that the geometric capacitances, $C^{geo}_{membrane}$ is depending on the applied voltages, $\Delta V_{membrane}$ as equation 1: $C^{geo}_{membrane} = \frac{\sigma}{\Delta V_{membrane(t)}} = \frac{\varepsilon_r \varepsilon_0}{d_{membrane(t)}}$ **(1)** Where σ is the surfaces charges densities of a specific membrane, and ε_0 is the permittivity of free spaces around ~8.85×10^{-12} F.m$^{-1,}$ and $d_{membrane(t)}$ is the thickness expectation filling through the alkyl chains as a dielectric of the various phospholipids such as DPPC, DOPG, DOPE, DOPS and DMPC. They are also a function of time due to dynamic behavior. In this work, a part of cell membrane is modeled such as capacitor through creating the insulating layers of alkyls between two phosphates group. With assuming which the two side of membranes carry $\pm$Q charges from one phospholipids towards the opposite phospholipids, the initial energies have been stored in the an electrostatic fields between two side of membrane as the capacitors which it can be given by the equation as follows $E_i = \frac{Q^2}{2C}$ **(2).**

Via allowing the electrons (based on tunneling effect) inside the insulating layers from the negative side to the positive side, the charges (Q+Δq) resides on the top electrodes and (−Q −Δq) resides on the bottom electrodes, the stored energies in this position can be estimated as $E_f = \frac{(Q+\Delta q)^2}{2C}$ **(3).** It is notable that the charges theme selves are quantized, and also polarized therefore the energies cannot be stored on the membrane sides before a single electron tunnels through the phospholipid's alkyl layer from the positive side to the negative side and stored energy can be written as: $\Delta E_s = E_f - E_i = \frac{\Delta q(Q+\frac{\Delta q}{2})}{C}$ **(4).** In these conditions, the larger voltages are in the ranges of $-\frac{\Delta q}{2C} < \Delta V < +\frac{\Delta q}{2C}$ **(6)**which the tunneling currents would only flow if the voltages are enough larger, i.e. $|\Delta V| > |\frac{q_e}{2C}|$ **(5)**. These effects are known as the coulomb blockades [25]. Obviously, the expectation distances of the spaces among the phospholipids sides of the membrane capacitor (d) should be sufficiently small such that the tunneling effect can be occurs for the suitable sizes in the cell membranes. In the macroscopic systems and for a small capacitor in the ranges of C~10^{-14} F, it can be exhibited that the voltages of $|\Delta V| > 1.5\mu V$ are needed for any tunneling effects for occurring. For the Nano-scales capacitors with capacitances in the ranges of "C ~ 10^{-17} F", the amount of $|\Delta V| > 1.5mV$ and for the Nano scales capacitors with the ranges of "C ~ 10^{-19} F" the amount of $|V| > 0.73V$ are needed to have a tunneling effect. In this condition columbine blockades are not apparent in macro-scaled circuits due to the low charging energies [25]. However, it might be occurred in Nano-scale due to the effects of the charging quantization. For micro systems, the capacitances might be so trivial that to be able of the charging energies ($\frac{e^2}{2C}$) **(7)** become large and consequently the energies value for tunneling effect into the quantum systems increase. It can be assumed the tunneling resistances to be $R_{Tun} = \frac{\Delta V}{I}$ **(8)** anyway; they theoretically allow the electrons to cross the insulating junction as discrete occurrences which "I" is the resulting currents due to the tunneling effects. These tunneling resistances are not normal resistances and allow the electrons to cross the insulating junction during "t=$R_{Tun}C_Q$" **(9)** which C_Q is the quantum capacitances. TheR_{Tun}, must be finite, so those tunneling effects might be practically take places. In these cases, the charges are said to be well quantized and the capacitors are considered to be a tunneling junction in thickness of membranes.

By this investigation, the $R_{Tunlling}$ for the membranes as a function of the thicknesses and differences in potential energies barrier among the electrodes through the uncertainty relationship between time and energy can be explained as. $\Delta E\, \Delta t \geq \frac{\hbar}{2} \rightarrow R_{Tun} \geq \frac{h}{2\pi q_e^2}$ **(10).** The hybrid of classical and quantum capacitances the net capacitances,C_{net}, can be calculated through the relation $\frac{1}{C_{net}} = \frac{1}{C_g} + \frac{2}{C_Q}$ **(11)** here C_Q is much more greater than the C_g. Therefore, these effects must only appear in the quantum systems such as cell membrane. In the fluid mosaics of lipids in the membranes, the dielectric constants changes time to time, while the changing in capacitances are not rapid and depend on the membrane processing situation.

2.2. Computational details.

Part of the phospholipids including DPPC, DOPG, DOPE, DOPS and DMPC has been simulated with QM/MM methods from ONIOM calculation which are accomplished with Monte Carlo (MC) estimation and various force fields such as OPLS, Amber and Charmm. The model contains 80 phospholipids. Each of 80 DPPC phospholipids, were handled with the lateral dimensions of the simulation cells [L_x], [Ly] and [L_z] such that the area per molecule was 59.5, 62.5 and 65.5 Å. The pressure was fixed through variants of the extended systems formalism and the

Langevin algorithms, which reduce oscillation in the cell parameter. The temperature was chosen at 300 K which corresponds to the biological system and identical to the relevant experiment. Structures of each lipid in 80 numbers consistent via a mean field generated through MC simulation for obtaining corresponding with experimental parameters. In this work, various force fields are used via comparing the calculated energies and the Hyper-Chem professional 7.01 programs are selected for any necessary additional calculations. The final characterizations of phospholipids were computed using self-consistent field theory for estimating optimal geometries, as well as the partial charge. The DFT with the van der Waals densities were applied for modeling the exchange-correlation energies of DPPC, DOPG, DOPE, DOPS and DMPC monomers and all optimization of these monomers were accomplished via Gaussian 98 [26]. The results from DFT methods such as m062x, m06-L, and m06 for the (DPPC, DOPG, DOPE, DOPS and DOPE)$_n$ {n=1-16} for 80 phospholipids were obtained. The m062x, m06-L and m06-HF are most practical DFT functional with a suitable agreement in non-bonded estimation between those monomers [27].

The ONIOM method consists of three sections of 1-high (H), 2-medium (M), and 3-low (L) has been accomplished for estimating the non-bonded interactions among DPPC, DOPG, DOPE, DOPS and DOPE monomers. Therefore tight DFT method is used for the H level and pm6 which is a semi empirical command is used for M (with pseudo=lanl2) and in the third the Pm3MM which is an order of Molecular mechanics was used for low (L) level. In addition, the semi empirical approach has been used for estimating the non-bonded energies among of upper lateral phospholipids side (P_+) and lower lateral phospholipids side (P_-). Generalized gradient approximation (GGA) from Perdew works [28] has been used for calculation exchange-correlation functional for all systems. Electrostatic potential-derived from charges potential (ESP) for head groups of DPPC, DOPG, DOPE, DOPS were run using chelp-G of Merz, Kollman and Singh methods[29]. Sometimes the MESP fitting is not suitable for treating macromolecules whereas in some parts innermost atoms are located far away from the center of MESP starting. Therefore, the innermost atomic charges will not considerable change outside of the macromolecule, in other words the accurate values for the innermost atomic charge is not well-calculated through MESP outside the macromolecule. In these items the representative charges should be computed as average values over several macromolecular conformations. A detailed explanation of the basis sets and the Hamiltonian for the charges distribution can be studied in references 30 to 37 [30-37]. The charge densities diagram has been summarized from first-principles approaches via an averaging calculating and the interaction energies for capacitors were defined according to the following equation. $E_S(eV) = \{E_C -$
$(\sum_{i=1}^{40}(\text{DPPC, DOPG, DOPE, DOPS}_+)_i +$
$\sum_{i=1}^{40}(\text{DPPC, DOPG, DOPE, DOPS}_-)_i)\}+E_{BSSE}$ **(12)** which "ΔE_S" is the stabilities energies of membrane capacitors. Electron densities data of wave-functions, electrons spin densities, electrostatic potentials, electron localization functions (ELF), localized orbitals locators (LOL) defined by Becke & Tsirelson [38], ESP and the averages local ionization energies using the Multifunctional Wave-function analyzer have also been performed [39]. Some parts of our strategy for various methods are explained in some of our previous works [40-60]

3. RESULTS

The 80 phospholipids of each DPPC, DMPC, DOPG, DOPE, DOPS molecules which include various atoms (an instance for DPPC=50 atoms) are selected and shown in Fig.3&4. In the tables 1&2, the physical and electrical properties from changing the internal conformation of those lipids are listed. Electron densities, energy densities and Potential energy densities for angular rotation of α, β and γ are calculated and exhibited from the angular distributions of each model (Table 1).

If the electrons are completely localized in phospholipids, they can be distinguished from the ones outside. As shown in table 1, the regions with large electron localization have large magnitudes of LOL which can lead the phospholipids towards upper lateral membrane side (P_+) with excess electrons and lower lateral membrane side (P_-) with excess holes. ELF exhibits that it is truly a comparative localization and should be accounted with the ranges of [0, 1]. A largest ELF value corresponds to the largest localized electron that shows the covalent bonds. Similar to ELF in term of kinetic energies, though; LOL can also be interpreted in term of localized functions. Small or large LOL value often appears in the inner boundary zone of localized orbital due to the large or small gradients of orbital's wave-function in this region. The value ranges of LOL are identical to ELF, namely [0, 1].

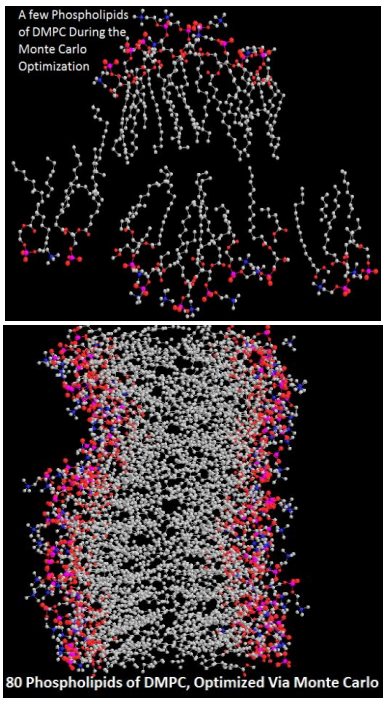

Figure 3. DMPC optimization in a model of membrane including of 80 DMPC via Monte Carlo calculation.

LOL have similar compare to ELF. As it is shown in table 1, LOLs are low and constant for both lateral and membrane sides ($P_{\pm}$). The result of ELF or LOL exhibit the phospholipid membrane starts for acting as Bio- capacitor in various scales from Nano to micro. As it is indicated in the Figure 4, the angles α, β and γ are shown and their distribution in the capacitor model is independent of the free space between the two layers in dynamic fluid Mosaic condition.

This free space (Fig.5) is a suitable distance for coulomb blockade and tunneling effects. Obviously, the free surfaces area increases and the membrane gets enough thin for maintaining the same places for the alkyl chains. The calculated data of dielectric constant for 80 phospholipids including DMPC, DPPC, DOPG, DOPE and DOPS of the membranes are listed in table 3.

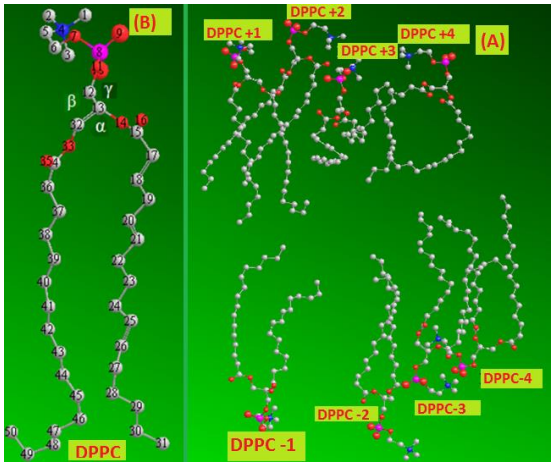

Figure 4. DPPC Optimization in a model of Membrane with α, β and γ Angles and 4 DPPC in two sides of membrane.

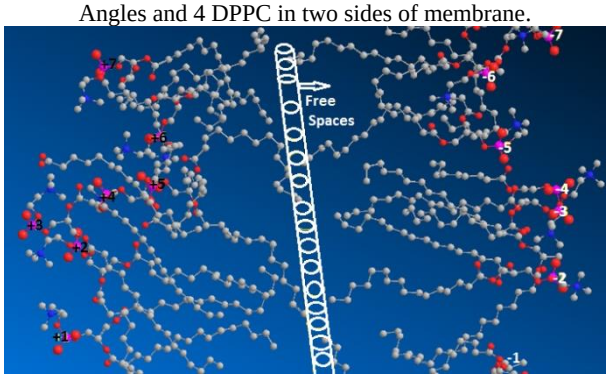

Figure 5. Free space between two layers in a dynamic situation, It is suitable space for electron tunneling in a coulomb blockade.

Head group area and the lateral diffusion coefficient for motion parallel for the DPPC can be calculated, based on references of 61, respectively [61]. As shown in figures 3-5, the peak spacing increases as the surfaces area decreases. Nagle [62] exhibited an occupied area, by hydrocarbon, arising from the lower electron densities of the terminal methyl group.

Table 1. Angles, ELF, LOL and ESP of Phosphor in DMPC, DOPG, DOPS.

Phospholipids & Number	ΔE_S (eV)	$ELF * LOL \dagger ESp\#$		$\alpha^{\circ}_{\pm n}, \beta^{\circ}_{\pm m}, \gamma^{\circ}_{\pm k}$	
$\mathbf{1_+}$ **(DMPC)**	0.0	P_{1_+}	1.44 (E-04)* 1.22 (E-02)† 7.14 (E+01)#	P_{1_+}	113.0° 111.3° 110.6°
$\mathbf{1_+,1_-}$ **(DOPG)**	+2.9	$P_{1_+}:P_{1_-}$	1.05: 1.06 (E-04)* 1.55: 1.41 (E-02)† 6.12: -6.14 (E+01)#	$P_{1_+}:P_{1_-}$	113.0:113.2 111.4:111.8 113.7:111.8
$\mathbf{2_+,2_-}$ **(DOPS**	+1.9	$P_{2_+}:P_{2_-}$	1.28:1.22 (E-04)* 1.15:1.17(E-02)† 5.83:-6.04 (E+01)#	$P_{2_+}:P_{2_-}$	113.0:113.2 111.3:111.8 113.6:113.9

These results correspond with the dielectric thickness of phospholipids distances in two sides of the membrane as a capacitor. If the electron densities profile varies along the two sides, additional intensities will appear. In this system of phospholipid bilayers this item does not create problems since the phospholipid molecules are located close to the nearest another. For building a model of bilayers of phospholipids, it is supposed which the CH_2 and CH3 terminal groups of the hydrocarbon fatty acids chains fill enough the spaces in the center of these bilayers and is also symmetrical. Therefore each group is considered for having the same volume as it occupied in the liquid hydrocarbons.

Table 2. Angles, ELF, LOL and ESP of Phosphor for OPE.

Phospholipids and Number	$ELF * LOL \dagger ESp\#$		$\alpha^{\circ}_{\pm n}, \beta^{\circ}_{\pm m}, \gamma^{\circ}_{\pm k}$	
$\mathbf{1_+,1_-}$	$P_{1_+}:P_{1_-}$	1.15: 1.16 (E-04)* 1.13: 1.12 (E-02)† 5.12:- 5.33 (E+01)#	$P_{1_+}:P_{1_-}$	113.0:113.2 111.5:111.7 113.4:113.9
$\mathbf{2_+,2_-}$	$P_{2_+}:P_{2_-}$	1.14:1.19 (E-04)* 1.18:1.08(E-02)† 6.13:-6.18 (E+01)#	$P_{2_+}:P_{2_-}$	113.3:113.1 111.2:111.7 111.5:111.4
$\mathbf{3_+,3_-}$	$P_{3_+}:P_{3_-}$	1.17:1.16 (E-04)* 1.06:1.08 (E-02)† 7.18:-7.59 (E+01)#	$P_{3_+}:P_{3_-}$	111.3:111.4 111.7:111.9 112.2:112.3
$\mathbf{4_+,4_-}$	$P_{4_+}:P_{4_-}$	1.15:1.14 (E-04)* 1.16:1.07 (E-02)† 7.14:-7.35 (E+01)#	$P_{4_+}:P_{4_-}$	113.5:113.4 111.1:111.5 113.3:113.2
$\mathbf{5_+,5_-}$ **(DOPE)**	$P_{5_+}:P_{5_-}$	1.15:1.13 (E-04)* 1.07:1.02 (E-02)† 6.43:-6.82 (E+01)#	$P_{5_+}:P_{5_-}$	113.5:112.9 111.5:111.4 111.3:111.8

The volume of the head group is a summation of the atomic radios which can be derived for phospholipids in solution. Head group of electron densities is higher than that of water, while the fatty acid chain forms a suitable layer with lowest electrons densities than that of water. The fatty acid chains layer gives negative amplitudes which decrease quickly. In this work, DMPC, DPPC, DOPG, DOPE and DOPS were chosen as membrane capacitors since the chain alkyl groups have excellent spaces filling, similar to that of biological systems. As the alkyls chains in phospholipids cells present ideal electrical insulator that can be polarized via applying an external electrical fields, the expected thickness of alkyl layers between the membrane plates with a dynamical behavior (fluid mosaic) model has been calculated and optimized and applied as a suitable simulation of dielectrics for capacitances (Table3).

Table 3. Dielectric constant, different voltages, capacitance and the stability energies of various modeled membrane capacitors in various thicknesses.

Phospholipids & Number	ΔE_S (eV)	$\Delta V = \Delta(\sum V_{P_+}^{1toN} \sum V_{P_-}^{1toN})$	$\Delta Q = \Delta(\sum Q_{P_+}^{1-N} - \lvert \sum Q_{P_-}^{1-N} \rvert)$	Dielectric Constant
DOPG (80)	0.22	5.33	1.66	7.32
DPPC (80)	+0.42	5.13	1.25	8.23
DMPC (80)	+1.1	3.21	1.21	6.45
DOPE (60)	0.85	7.31	1.43	4.13

Phospholipids & Number	ΔE_S (eV)	$\Delta V = \Delta(\sum V_{P_+}^{1toN} \sum V_{P_-}^{1toN})$	$\Delta Q = \Delta(\sum Q_{P_+}^{1-N} - \lvert \sum Q_{P_-}^{1-N} \rvert)$	Dielectric Constant
DOPS (60)	+0.65	8.41	1.36	5.81

The structural and mechanical definition of the systems and also its performance in the simulation of the capacitor model can be discussed in the biological mechanism in membrane functions. As instance, the ESP value approximately is constant (Table 1&2) which means the variable capacitances in membranes are independent of a number of phospholipids. This subject indicates what makes the cell membrane for acting as a variable capacitor does not depend on the internal structural items such as the number of phospholipids. In contrast what makes the cell membrane for acting as variable capacitors might be related to the external cellular condition. The interaction energies among the several of two sides of membranes are also calculated. The dielectric permittivity as a function of dielectric constant depended on their sizes was determined using abinito calculations (Table 1&2).

The obtained data of the phospholipid structures such as the distances between two layers of membrane, dielectric permittivity of the chain alkyls, differences value of the charges on both sides, electrostatic magnitude using the SCF densities, fitting points charges data from ESP fitting, the stabilities energies of the various capacitors (eV), thickness consist of the net capacitances and also the potential differences between two electrodes of those membranes upper and lower lateral sides are listed in tables 2-4.

Table 4. The capacitance C_Q= quantum capacitance, C_g= geometry capacitance, and C_{net}= net capacitance, of modeled capacitors in various thicknesses

Phospholipids & Number	$C_Q(F) \times 10^{19}$		$C_{net}(F) \times 10^{19} = \frac{C_g C_Q}{C_Q + 2C_g}$	
	ESP	Mulliken	ESP	Mulliken
DOPG (80)	1.21	1.78	1.20	1.28
DPPC (80)	1.35	1.98	0.93	0.98
DMPC (80)	1.32	1.43	1.07	1.21
DOPE (60)	1.28	1.66	0.91	0.95
DOPS (60)	1.29	1.88	1.23	1.44

The potential energies differences between the two upper and lower lateral sides, $\Delta V = \Delta(\sum V_{P_+}^{1toN} - \sum V_{P_-}^{1toN})$ (a.u.) varies between 3.21 and 8.41 volts for the various membrane. It is notable that for obtaining the inter-layers attractions the QM/MM methods with an ONIOM approaches have been applied including several forces fields. Therefore the number of alkyl chains, volumes of the head groups, area for the upper and lower lateral sides (P_+, P_- sides) have been obtained as $A \approx \alpha \times 10^{-21}$ m^2 up to $\alpha \times 10^{-20}$ m^2 depends on condition of membranes. The Nano-capacitances of several membranes (C_g, C_Q and C_{net}) are listed in table 3. It is notable that for alkyls chains spaces filler containing several layers, the differences voltages between upper and lower lateral sides (P_+, P_- sides) would be related on several conditions such as non-equilibrium states and dynamic situations of the coupling between each phospholipids and adjacent one, etc. Although for the Nano-scale membranes capacitors, the different voltages and then dielectric constants can be estimated from the band gap or ECP calculations, for large dielectric thicknesses, the classical capacitances obey from the rule of the "$C_g \propto \frac{1}{d}$". These adaptabilities are not valid for short distances, which is attributed to the quantum effects. The dielectric permittivity as a function of dielectric sizes can be calculated from the equation as follows, $C_Q(F) \times 10^{20} = \frac{\Delta q(Q+\frac{\Delta q}{2})}{\Delta E_S}$ and $C_{net}(F) \times 10^{20} = \frac{C_g C_Q}{C_Q + 2C_g}$. The quantum effects for calculating the capacitances through $R_{Tun}(K\Omega) \gg \frac{\hbar}{\Delta_{ESP}^2}$, using the QM/MM methods are discussed and listed (tables 2 & 3). The quantum effect has appeared in a small region of the membrane's thickness due to type and number of phospholipid bi-layers in a membrane. considering the Heisenberg rule, some micro position of membrane's type capacitors are allowed to quantum tunneling, while some others are not which the reason of this phenomenon are not known yet. In an external field which produces via trance membrane proteins or ions the charges employ those forces that can influence the state of the membrane; consequently influencing the magnitude of the variable fields makes an amount of variable capacitances. These effects allow one for introducing a capacitive susceptibility that can be resonates with self-induction effect of helical coils in G proteins. Table 5 indicates the calculated helical proteins self-induction (of some G-proteins component) [63-74] through resonance with capacitances of several phospholipids membranes.

Table 5. Approximate self-induction of several membranes modeled capacitors with G-protein components.

membrane	
DOPG	60 GHZ
DPPC	50 GHZ
DMPC	55 GHZ
DOPE	56 GHZ
DOPS	65GHZ

Due to the greater inductance compared to conductance in coils, the helical coils of DNA, mRNA, and trance membrane proteins can be resonate with a capacitive susceptibility of phospholipids capacitors in biological phenomenon. When the proteins are coiled, the magnetic fields produced by current flow expands across adjacent the coil ring. Based on the current changing, the created induced magnetic fields also must be changed theoretically. This changing create enough forces that based on Lenz rule is opposed to the current changing. These effects do not occur in a static condition, though, it only arises in a variable of membrane capacitor during the current experiences suitable and enough changing in its value. When current flows rapidly, the magnetic field also collapses quickly and obviously is capable to generate a high induced electro-motor-forces and voltages at a short time. Membrane consisting of helical proteins as electrical inductors might enable the cell to transiently produce very high electrical voltages.

4. CONCLUSIONS

The cellular electrical properties and electromagnetic field's effects on cells result from the electro-biological phenomenon, such as ligand receptor interactions of hormones, alteration of mineral entry through the cell membrane and activation or inhibition of cytoplasmic enzyme reactions. Bio-membrane can be considered as thin capacitors with the unique feature of biological energies storages in a physiological phenomenon. Increasing the electrical potentials and capacitances of various membranes alters the dipole orientation, activation of helical proteins, DNA helix, increasing the codon transcription and translation and activating the cell membrane receptors that act as antennas for certain ranges of frequency and amplitude leading to the concepts of electromagnetic reception, transduction and attunement. The electrical fields from membrane capacitors induce dipole movements where the latter is a function of polarizability and also the strength of the electrical fields. When a biological phenomenon is exposed to an electrical field in the right frequency, a preferential alignment of dipoles becomes established. Since the cell membrane contains many dipole molecules, an electric field results in preferential alignment in the dipoles. This may be the mechanism in which the electrical fields alter membrane permeability and membrane functions. Resonance communication mechanisms depend on the interaction between membrane capacitors and helical proteins.

5. REFERENCES

1. Oldham, W.M.; Hamm, H.E. Structural basis of function in hetero-trimeric G proteins. *Q RevBiophys* **2006**, *39*, 117–66, https://doi.org/10.1017/S0033583506004306.
2. Calvert, P.D.; Strissel, K.J.; Schiesser, W.E.; Pugh, E.N.Jr.; Arshavsky, V.Y. Light-driven translocation of signaling proteins in vertebrate photoreceptors. *Trends Cell Biol* **2006,** *16*, 560–8, https://doi.org/10.1016/j.tcb.2006.09.001.
3. Tesmer, V.M.; Kawano, T.; Shankaranarayanan, A.; Kozasa, T.; Tesmer, J.J. Snapshot of activated G proteins at the membrane: the Galphaq-GRK2-Gbetagamma complex. *Science* **2005,** *310*, 1686–90, https://doi.org/10.1126/science.1118890.
4. Rask-Andersen, M.; Almén, M.S.; Schiöth, H.B.; Trends in the exploitation of novel drug targets. *Nat. Rev. Drug Discov* **2011,** *10*, 579–590, https://doi.org/10.1038/nrd3478.
5. Neves, S.R.; Ram, P.T.; Iyengar, R. G protein pathways. *Science* **2002**, *296*, 1636–1639, https://doi.org/10.1126/science.1071550.
6. Milligan, G.; Kostenis, E. Heterotrimeric G-proteins: a short history. *Br. J. Pharmacol* **2006**, *147*, 46–55, https://doi.org/10.1038/sj.bjp.0706405.
7. Rasmussen, S.G.F.; DeVree, B.T.; Zou, Y.; Kruse, A.C.; Chung, K.Y.; Kobilka, T.S. Crystal structure of the β2 adrenergic receptor-Gs protein complex. *Nature* **2011**, *477*, 549–555, https://doi.org/10.1038/nature10361.
8. Oates, J.; Watts, A. Uncovering the intimate relationship between lipids, cholesterol and GPCR activation. *Curr. Opin. Struct. Biol* **2011**, *21*, 802–807, https://doi.org/10.1016/j.sbi.2011.09.007.
9. Hauser, A.S.; Attwood, M.M.; Rask-Andersen, M.; Schiöth, H.B.; Gloriam, D.E. Trends in GPCR drug discovery: New agents, targets and indications. *Nat. Rev. Drug Discov* **2017**, *16*, 829–842, https://doi.org/10.1038/nrd.2017.178.
10. Redman, L.M.; Smith, S.R.; Burton, J.H.; Martin, C.K.; Il'yasova, D.; Ravussin, E. Metabolic Slowing and Reduced Oxidative Damage with Sustained Caloric Restriction Support the Rate of Living and Oxidative Damage Theories of Aging. *Cell Metab* **2018,** *27*, 805–815, https://doi.org/10.1016/j.cmet.2018.02.019.
11. van Meer, G.; Voelker, D.R.; Feigenson, G.W. Membrane lipids: where they are and how they behave. *Nat. Rev. Mol. Cell Biol*. **2008**, *9*, 112–124, https://doi.org/10.1038/nrm2330.
12. Hauser, A.S.; Attwood, M.M.; Rask-Andersen, M.; Schiöth, H.B.; Gloriam, D.E. Trends in GPCR drug discovery: New agents, targets and indications. *Nat. Rev. Drug Discov* **2017**, *16*, 829–842, https://doi.org/10.1038/nrd.2017.178.
13. Rosenbaum, D.M.; Rasmussen, S.G.; Kobilka, B.K. The structure and function of G-protein-coupled receptors. *Nature* **2009,** *459*, 356–363, https://dx.doi.org/10.1038%2Fnature08144.
14. Xiao, P.; Huang, X.; Huang, L.; Yang , J.; Li, A.; Shen, K.; Wedegaertner, P.B.; Jiang, X. G protein-coupled receptor kinase 4-induced cellular senescence and its senescence-associated gene expression profiling. *Exp. Cell Res* **2017**, *360*, 273–280, https://doi.org/10.1016/j.yexcr.2017.09.017.
15. Luttrell, L.M.; Maudsley, S.; Gesty-Palmer, D. Translating in vitro ligand bias into in vivo efficacy. *Cell Signal* **2018**, *41*, 46–55, https://doi.org/10.1016/j.cellsig.2017.05.002.
16. Luttrell, L.M.; Gesty-Palmer, D. Beyond desensitization: Physiological relevance of arrestin-dependent signaling. *Pharmacol. Rev* **2010**, *62*, 305–330, https://doi.org/10.1124/pr.109.002436.
17. Hara, M.R.; Sachs , B.D.; Caron, M.G.; Lefkowitz, R.J. Pharmacological blockade of a β(2)AR-β-arrestin-1 signaling cascade prevents the accumulation of DNA damage in a behavioral stress model. *Cell Cycle* **2013,** *12*, 219–224, https://doi.org/10.4161/cc.23368.
18. Whorton, M.R.; Bokoch, M.P.; Rasmussen, S.G.; Huang, B.; Zare, R.N.; Kobilka, B.; Sunahara, RK. A monomeric G protein-coupled receptor isolated in a high-density lipoprotein particle efciently activates its G protein. *Proc. Natl. Acad. Sci. USA* **2007**, *104*, 7682–7687, https://doi.org/10.1073/pnas.0611448104.
19. Dawaliby, R.; Trubbia, C.; Delporte, C.; Masureel, M.; antwerpen, P.V.; Kobilk, B.K.; Govaerts, C. Allosteric regulation of G protein-coupled receptor activity by phospholipids. *Nature Chemical Biology* **2015**, *11*, 1-4, https://doi.org/10.1038/nchembio.1960.
20. Rasmussen, S.G.; DeVree, B.T.; Zou, Y.; Kruse, A.C.; Chung, K.Y.; Kobilka, T,S.; Thian, F.S.; Chae, P.S.; Pardon, E.; Calinski, D.; Mathiesen, J.M.; Shah, S.T.; Lyons, J.A.; Caffrey, M.; Gellman, S.H. Steyaert, J.; Skiniotis, G.; Weis, W.I.; Sunahara, R.K.; Kobilka, B.K. Crystal structure of the β2 adrenergic receptor-Gs protein complex. *Nature* **2011**, *477*, 549–555, https://doi.org/10.1038/nature10361.
21. Hanson, M.A.; Roth, C.B.; Jo, E.; Griffith, M.T.; Scott, F.L.; Reinhart, G.; Desale, H.; Clemons, B.; Cahalan, S.M.; Schuerer S.C.; Sanna, M.G.; Han, G.W.; Kuhn, P.; Rosen, H.; Stevens, R.C. Crystal structure of a lipid G protein-coupled receptor. *Science* **2012,** *335*,851-855, https://doi.org/10.1126/science.1215904.
22. Roark, M.; Feller, S.E. Molecular Dynamics Simulation Study of Correlated Motions in Phospholipid Bilayer Membranes. *J. Phys. Chem. B* **2009**, *113*, 13229–13234, https://doi.org/10.1021/jp902186f.

23. Smith, C.W. Superconducting areas in living systems. In *R. K. Mishra (Ed.), The living state II Singapore: World Scientific*, 1985; 404-420.
24. Choy, R.V.S.; Monro, J.A.; Smith, C.W. Electrical senitivities in allergy patients. *Clin. Ecol*. **1986**, *4*, 93-102.
25. Klein, D.L.; Roth, R.; Lim, A.K.L.; Alivisatos, A.P.; McEuen, P.L. A single-electron transistor made from a cadmium selenide nano-crystal. *Nature (London)* **1997**, *389*, 699, https://doi.org/10.1038/39535.
26. Frisch, M.J.; Trucks, G.W.; Schlegel, H.B.; Scuseria, G.E.; Robb, M.A.; Cheeseman, J.P.; Zakrzewski, V.G.; Head-Gordon, M.; Replogle, E.S.; Pople, J.A. Gaussian 98, *Gaussian, Inc., Pittsburgh, PA*, 1998**.**
27. Zhao, Y.; Truhlar, D.G. The M06 suite of density functionals for main group thermochemistry, thermochemical kinetics, noncovalent interactions, excited states, and transition elements: two new functionals and systematic testing of four M06-class functionals and 12 other functionals. *Theor Chem Account* **2008,** *120*, 215–241**,** https://doi.org/10.1007/s00214-007-0310-x.
28. Perdew, J.P.; Burke, K.; Ernzerhof. Generalized Gradient Approximation Made Simple. *Phys. Rev. Lett*. **1996**, *77*, 3865-3868, https://doi.org/10.1103/PhysRevLett.77.3865.
29. Besler, B.H.; Merz, K.M.; Kollman, PA. Atomic charges derived from semiempirical methods. *J. comp. Chem*. **1990,** *11* 431, https://doi.org/10.1002/jcc.540110404.
30. Mollaamin, F.; Najafpour, J.; Ghadami, S.; Akrami, M.S.; Monajjemi, M. The Electromagnetic Feature of B15N15Hx (x=0,4, 8, 12, 16, and 20) Nano Rings: Quantum Theory of Atoms in Molecules/NMR Approach. *Journal of computational and theoretical nanoscience* **2014**, *11*, 1290-1298.
31. Monajjemi, M.; Ahmadianarog, M. Carbon Nanotube as a Deliver for Sulforaphane in Broccoli Vegetable in Point of Nuclear Magnetic Resonance and Natural Bond Orbital Specifications. *Journal of computational and theoretical nanoscience* **2014**, *11*, 1465-1471, https://doi.org/10.1166/jctn.2014.3519.
32. Monajjemi, M.; Mahdavian, L.; Mollaamin, F. Characterization of nanocrystalline silicon germanium film and nanotube in adsorption gas by monte carlo and langevin dynamic simulation. *Bulletin of the chemical society of Ethiopia* **2008**, *22*, 277-286, http://dx.doi.org/10.4314/bcse.v22i2.61299.
33. Monajjemi, M.; Ghiasi, R.; Ketabi, S.; Pasdar, H.;Mollamin, F. A theoretical study of metal-stabilised rare tautomers stability: N4 metalated cytosine (M=Be2+, Mg2+,Ca2+, Sr2+ and Ba2+) in gas phase and different solvents. *Journal of chemical research* **2004**, *1*, 11-18, https://doi.org/10.3184/030823404323000648.
34. Monajjemi, M.; Ghiasi, R.; Sadjadi, M.A.S. Metal-stabilized rare tautomers: N4 metalated cytosine (M = Li+, Na+, K+, Rb+ and Cs+), theoretical views. *Applied organometallic chemistry* **2003**, *17*, 635-640, https://doi.org/10.1002/aoc.469.
35. Monajjemi, M.; Mahdavian, L.; Mollaamin, F.;Honarparvar, B. Thermodynamic Investigation of EnolKeto Tautomerism for Alcohol Sensors Based on Carbon Nanotubes as Chemical Sensors. *Fullerenes nanotubes and carbon nanostructures* **2010**, *18*, 45-55, https://doi.org/10.1080/15363830903291564.
36. Hadad, B.K.; Mollaamin, F; Monajjemi, M. Biophysical chemistry of macrocycles for drug delivery: a theoretical study. *Russian chemical bulletin* **2011**, *60*, 238-241, https://doi.org/10.1007/s11172-011-0039-5.
37. Monajjemi, M.; Honaparvar, B.; Hadad, B.K.; Ilkhani, A.R.; Mollaamin F. Thermo-chemical investigation and NBO analysis of some anxileotic as Nano- drugs. *African journal of pharmacy and pharmacology* **2010**, *4*, 521-529.
38. Becke, A.D.; Edgecombe, A. simple measure of electron localization in atomic and molecular systems. *The Journal of Chemical Physics* **1990**, *92*, 5397-5403, https://doi.org/10.1063/1.458517.
39. Lu, T.; Chen, F. Multiwfn: A Multifunctional Wavefunction Analyzer. *J. Comp. Chem*. **2012**, *33*, 580-592, https://doi.org/10.1002/jcc.22885.
40. Monajjemi, M.; Naderi, F.; Mollaamin, F.; Khaleghian, M. Drug Design Outlook by Calculation of Second Virial Coefficient as a Nano Study. *Journal of the mexican chemical society* **2012**, *56*, 207-211.
41. Monajjemi, M.; Mohammadian, N.T.S-NICS an Aromaticity Criterion for Nano Molecules. *J. Comput. Theor. Nanosci* **2015**, *12*, 4895-4914**.**
42. Monajjemi, M.; Lee, V.S.; Khaleghian, M.; Honarparvar, B.; Mollaamin, F. Theoretical Description of Electromagnetic Nonbonded Interactions of Radical, Cationic, and Anionic NH2BHNBHNH2 Inside of the B18N18 Nanoring. *J. Phys. Chem C* **2010**, *114*, 15315, http://dx.doi.org/10.1021/jp104274z.
43. Monajjemi, M.; Boggs, J.E.; A New Generation of BnNn Rings as a Supplement to Boron Nitride Tubes and Cages. *J. Phys. Chem. A* **2013**, *117*, 1670-1684, http://dx.doi.org/10.1021/jp312073q.
44. Monajjemi, M. Non bonded interaction between BnNn (stator) and BN B (rotor) systems: A quantum rotation in IR region. *Chemical Physics* **2013**, *425*, 29-45, https://doi.org/10.1016/j.chemphys.2013.07.014.
45. Monajjemi, M.; Robert, W.J.; Boggs, J.E. NMR contour maps as a new parameter of carboxyl's OH groups in amino acids recognition: A reason of tRNA–amino acid conjugation. *Chemical Physics* **2014**, *433*, 1-11, https://doi.org/10.1016/j.chemphys.2014.01.017.
46. Monajjemi, M. Quantum investigation of non-bonded interaction between the B15N15 ring and BH2NBH2 (radical, cation, and anion) systems: a nano molecularmotor. *Struct Chem* **2012,** *23*, 551–580, http://dx.doi.org/10.1007/s11224-011-9895-8.
47. Monajjemi, M. Non-covalent attraction of B2N (2, 0) and repulsion of B2N (+) in the BnNn ring: a quantum rotatory due to an external field. *Theor Chem Acc* **2015**, 1668-9, https://doi.org/10.1007/s00214-015-1668-9.
48. Monajjemi, M. Metal-doped graphene layers composed with boron nitride–graphene as an insulator: a nano-capacitor. *Journal of Molecular Modeling* **2014**, *20*, 2507, https://doi.org/10.1007/s00894-014-2507-y.
49. Ilkhani, A.R.; Monajjemi, M. The pseudo Jahn-Teller effect of puckering in pentatomic unsaturated rings C(4)AE(5), A = N, P, As, E = H, F, Cl. *Computational and theoretical chemistry* **2015**, *1074*, 19-25.
50. Monajjemi M. Graphene/(h-BN)*n*/X-doped raphene as anode material in lithium ion batteries (X = Li, Be, B AND N). *Macedonian Journal of Chemistry and Chemical Engineering* **2017**, *36*, 101–118, http://dx.doi.org/10.20450/mjcce.2017.1134.
51. Monajjemi, M.; Najafpour, J. Charge density discrepancy between NBO and QTAIM in single-wall armchair carbon nanotubes. *Fullerenes Nanotubes and Carbon Nanostructures* **2014**, *22*, 575-594, https://doi.org/10.1080/1536383X.2012.702161.
52. Monajjemi, M. Cell membrane causes the lipid bilayers to behave as variable capacitors: A resonance with self-induction of helical proteins. *Biophysical Chemistry* **2015**, *207*, 114 –127. https://doi.org/10.1016/j.bpc.2015.10.003.
53. Mollaamin, F.; Monajjemi, M. DFT outlook of solvent effect on function of nano bioorganic drugs. *Physics and*

Chemistry of Liquids **2012**, *50*, 596-604, https://doi.org/10.1080/00319104.2011.646444.
54. Monajjemi, M.; Chegini, H.; Mollaamin, F.; Farahani, P. Theoretical Studies of Solvent Effect on Normal Mode Analysis and Thermodynamic Properties of Zigzag (5,0) carbon nanotube. *Fullerens Nanotubes carbon and nanostructures* **2011**, *19*, 469-482, https://doi.org/10.1080/1536383X.2010.494783.
55. Monajjemi, M. Study of CD5+ Ions and Deuterated Variants (CHxD(5-x)+): An Artefactual Rotation. *Russian Journal of Physical Chemistry a* **2018,** *92*, 2215-2226.
56. Monajjemi, M.; Baei, M.T.; Mollaamin, F. Quantum mechanics study of hydrogen chemisorptions on nanocluster vanadium surface. *Russian journal of inorganic chemistry* **2008,** *53*, 1430-1437, https://doi.org/10.1134/S0036023608090143.
57. Monajjemi, M. Liquid-phase exfoliation (LPE) of graphite towards graphene: An ab initio study. *Journal of Molecular Liquids* **2017**, *230*, 461–472, https://doi.org/10.1016/j.molliq.2017.01.044.
58. Monajjemi, M.; Mahdavian, L.; Mollaamin, F. Interaction of Na, Mg, Al, Si with carbon nanotube (CNT): NMR and IR study. *Russian Journal of Inorganic Chemistry* **2009,** *54*, 1465-1473, https://doi.org/10.1134/S0036023609090216.
59. Monajjemi, M.; Ahmadianarog, M. Carbon Nanotube as a Deliver for Sulforaphane in Broccoli Vegetable in Point of Nuclear Magnetic Resonance and Natural Bond Orbital Specifications. *Journal of computational and theoretical nanoscience* **2014**, *11*, 1465-1471, http://dx.doi.org/10.1166/jctn.2014.3519.
60. Lee, V.S.; Nimmanpipug, P.; Mollaamin, F.; Kungwan, N.; Thanasanvorakun, S.; Monajjemi, M. Investigation of single wall carbon nanotubes electrical properties and mode analysis: Dielectric effects. *Russian journal of physical chemistry A* **2009**, *83*, 2288-2296, https://doi.org/10.1134/S0036024409130184.
61. Filippov, A.; Orädd, G.; Lindblom, G. Domain Formation in Model Membranes Studied by Pulsed-Field Gradient-NMR: The Role of Lipid Polyunsaturation. *Biophys. J*. **2007**, *93*, 3182– 3190, https://dx.doi.org/10.1529%2Fbiophysj.107.111534.
62**.** Nagle, S.T.; Petrache, H.I.; Nagle, J.F. Structure and interactions of fully hydrated dioleoylphosphatidylcholine bilayers. *Biophys J.* **1998**, *75*, 917–925, https://dx.doi.org/10.1016%2FS0006-3495(98)77580-0.
63. Jong, Y.I.; Harmon, S.K.; O'Malley, K.L. GPCR signaling from within the cell. *Br. J. Pharmacol.* **2017**, 1–10, https://doi.org/10.1111/bph.14023.
64. Jong, Y.I.; Harmon, S.K.; O'Malley, K.L. Intracellular GPCRs Play Key Roles in Synaptic Plasticity. *ACS Chem. Neurosci.* **2018**, https://doi.org/10.1021/acschemneuro.7b00516.
65. Maudsley, S.; Devanarayan, V.; Martin, B.; Geerts, H. Brain Health Modeling Initiative (BHMI). Intelligent and effective informatic deconvolution of "Big Data" and its future impact on the quantitative nature of neurodegenerative disease therapy. *Alzheimers Dement.* **2018**, *14*, 961–975, https://doi.org/10.1016/j.jalz.2018.01.014.
66. Palovcak, A.; Liu, W.; Yuan, F.; Zhang, Y. Maintenance of genome stability by Fanconi anemia proteins. *Cell Biosci.* **2017**, *7*, 8, https://doi.org/10.1186/s13578-016-0134-2.
67.Van Gastel, J.; Hendrickx, J.; Leysen, H.; Luttrell, L.M.; Lee, M.-H.M.; Azmi, A.; Janssens, J.; Maudsley, S. The RXFP3-GIT2 signaling system represents a potential multidimensional therapeutic target in age-related disorders. *FASEB J.* **2018**, *32*, 1.
68. Siddiqui, S.; Lustig, A.; Carter, A.; Sankar, M.; Daimon, C.M.; Premont, R.T.; Etienne, H.; van Gastel, J.; Azmi, A.; Janssens, J.; Becker, K.G.; Zhang, Y.; Wood, W.; Lehrmann, E.; Martin, J.G.; Martin, B.; Taub, D.D.; Maudsley, S. Genomic deletion of GIT2 induces a premature age-related thymic dysfunction and systemic immune system disruption. *Aging* **2017**, *9*, 706–740, https://doi.org/10.18632/aging.101185.
69. Herraiz, C.; Garcia-Borron, J.C.; Jiménez-Cervantes, C.; Olivares, C. MC1R signaling. Intracellular partners and pathophysiological implications. *Biochim. Biophys. Acta* **2017**, *1863*, 2448–2461, https://doi.org/10.1016/j.bbadis.2017.02.027.
70. Sun, X.; Shi, B.; Zheng, H.; Min, L.; Yang, J.; Li, X.; Liao, X.; Huang, W.; Zhang, M.; Xu, S. Senescence-associated secretory factors induced by cisplatin in melanoma cells promote non-senescent melanoma cell growth through activation of the ERK1/2-RSK1 pathway. *Cell Death Dis.* **2018,** https://doi.org/10.1038/s41419-018-0303-9.
71. Wagner, W.; Kania, K.D.; Blauz, A.; Ciszewski, W.M. The lactate receptor (HCAR1/GPR81) contributes to doxorubicin chemoresistance via ABCB1 transporter up-regulation in human cervical cancer HeLa cells. *J. Physiol. Pharmacol.* **2017**, *68*, 555–564.
72. Wagner, W.; Kania, K.D.; Ciszewski, W.M. Stimulation of lactate receptor (HCAR1) affects cellular DNA repair capacity. *DNA Repair* **2017**, *52*, 49–58, https://doi.org/10.1016/j.dnarep.2017.02.007.
73. Yong, M.; Yu, T.; Tian, S.; Liu, S.; Xu, J.; Hu, J.; Hu, L. DR2 blocker thioridazine: A promising drug for ovarian cancer therapy. *Oncol. Lett.* **2017**, *14*, 8171–8177, https://doi.org/10.3892/ol.2017.7184.
74. Wang, W.; Qiao, Y.; Li, Z. New Insights into Modes of GPCR Activation. *Trends Pharmacol. Sci.* **2018**, *39*, 367–386, https://doi.org/10.1016/j.tips.2018.01.001.

6. ACKNOWLEDGEMENTS

The Author Thanks IAU University, Central Tehran Branch for their supporting in Software and computer equipment.